Hindawi Publishing Corporation
Advances in Condensed Matter Physics
Volume 2011, Article ID 216065, 5 pages
doi:10.1155/2011/216065

Research Article

First-Principles Calculation on Initial Stage of Oxidation of Si (110)-(1 × 1) Surface

Takahiro Nagasawa and Koji Sueoka

Department of System Engineering, Okayama Prefectural University, 111 Kuboki, Soja, Okayama 719-1197, Japan

Correspondence should be addressed to Koji Sueoka, sueoka@c.oka-pu.ac.jp

Received 4 October 2010; Revised 24 December 2010; Accepted 7 February 2011

Academic Editor: Rosa Lukaszew

The initial stage of oxidation of an Si (110)-(1 × 1) surface was analyzed by using the first-principles calculation. Two calculation cells with different surface areas were prepared. In these cells, O atoms were located at the Si–Si bonds in the first layer (A-bonds) and at the Si–Si bonds between the first and second layers (B-bonds). We found that (i) the most stable site of one O atom was the A-bond, and (ii) an O (A-bond) –Si–O (A-bond) was the most stable for two O atoms with a coverage ratio of R_{ox} = 0.06 while an O (A-bond) –Si–O (B-bond) was the most stable for R_{ox} = 0.10. The stability of O (A-bond) –Si–Si–O (A-bond) was less than the structures obtained in (ii). The other calculations showed that the unoxidized A-bonds should be left when a coverage ratio of R_{ox} is close to 1. These simulations suggest that the O atoms will form clusters in the initial stage of oxidation, and the preferential oxidation will change from the A-bonds to the B-bonds up to the formation of 1 monolayer (ML) oxide. The results obtained here support the reported experimental results.

1. Introduction

The performance of electronic devices has been markedly improved with the development of microfabrication technology, which allows for the use of thin nanoscale Si films. However, as the improvements in scaling technology will reach their uppermost limit in the near future, alternative technology is required. There is a great deal of engineering interest in Si (110) wafers used as the substrates of large-scale integrations (LSI) for next generation technology because the hole mobility of (110) is higher than that of a (100) surface; about 2.5 times as high as that of (100) [1]. Despite this importance, few studies on Si (110) surface have been reported in comparison with other low-index surfaces. It was previously reported that the most stable configuration of a Si (110) clean surface was a (16 × 2) reconstruction at temperatures of less than about 700°C [2]. The detailed structure and initial oxidation of a Si (110)-(16 × 2) clean surface were experimentally [3–5] and theoretically [6, 7] studied by different research groups including us [7]. On the other hand, at temperatures higher than about 700°C, the Si (110)-(1 × 1) surface was the most stable [2]. Suemitsu et al. [8] experimentally studied the oxidation process up to 1 monolayer (ML) of the Si (110)-(1 × 1) surface and suggested the preferential oxidation of B-bonds (Si–Si bonds between the first and second layers). However, to the best of our knowledge, there have been few theoretical studies on the initial stage of oxidation on Si (110)-(1 × 1) surfaces.

In this paper, we analyzed the initial stage of oxidation on a Si (110)-(1 × 1) clean surface using the first-principles calculation. We calculated the total energy of the two geometrically optimized cells with different surface areas including O atoms at the Si–Si bonds in the first layer (A-bonds) and at the Si–Si bonds between the first and second layers (B-bonds). The obtained results were discussed with the reported experimental results.

2. Calculation Details

We used the CASTEP code of the first-principles calculation with the local density approximation (LDA) based on the density functional theory [9]. In this calculation, the Kohn-Sham equation was solved self-consistently in order to obtain the ground state of the system for given atomic configurations [10]. The wave functions were expanded with the plane waves, and the ultra-soft pseudopotential method

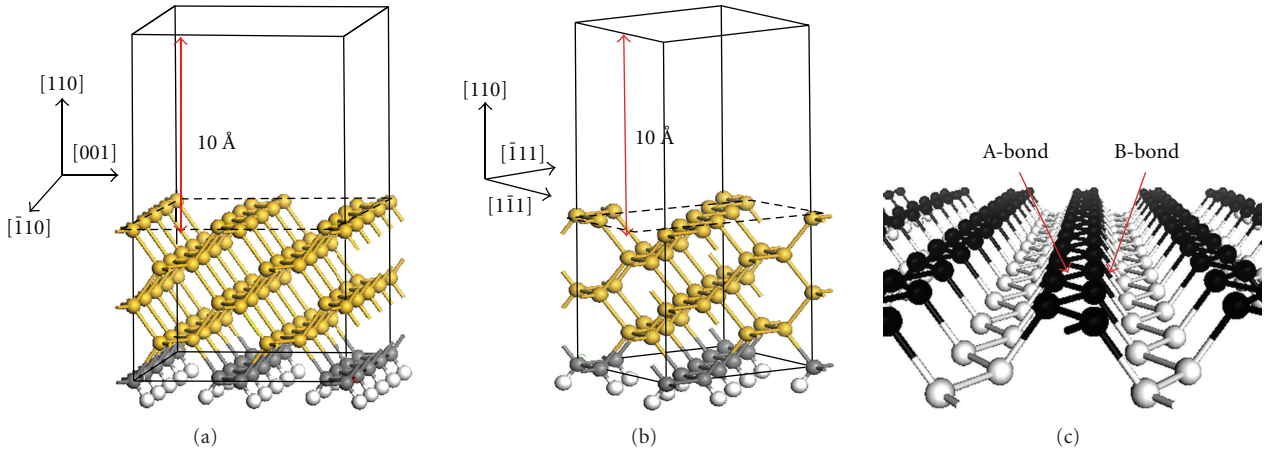

FIGURE 1: Calculation model of Si (110)-(1 × 1) surface: (a) *large model*, (b) *small model*, and (c) A-bond and B-bond. In (c), black (white) balls indicate the Si atoms in the first (second) layer.

[11] was used to reduce the number of plane waves. The cutoff energy was 340 eV. The expression proposed by Perdew et al. [12] was used for the exchange-correlation energy in the generalized gradient approximation (GGA). The density mixing method [13] and BFGS geometry optimization method [14] were used to optimize the electronic structure and configurations, respectively.

We prepared two simulation cells to analyze the (110)-(1 × 1) surface using different coverage ratios of the O atoms. One is the "*large model*" shown in Figure 1(a) with a rectangular surface area of about 200 Å^2 with [−1 1 0] and [0 0 1] edges. There were 80 Si atoms in this model. The other is the "*small model*" shown in Figure 1(b), which had a rhombus surface area of about 100 Å^2 with [1 −1 1] and [−1 1 1] edges. There were 40 Si atoms in this model. Figure 1(c) shows the atomic configuration of the Si (110)-(1 × 1) surface before the geometry optimization. Here, we define that the Si–Si bond of zigzag line in the first layer is an A-bond. The Si–Si bond between the first and second layers is defined as a B-bond.

In these analyses, we defined the coverage ratio of the O atoms, R_{ox}, using (1):

$$R_{ox} = \frac{N_O}{N_{Si-Si}}. \quad (1)$$

Here, N_O and $N_{Si\text{-}Si}$ indicate the number of O atoms and the sum of the A- and B-bonds on the surface in the simulation cell, respectively. When one O atom is included in each cell, R_{ox} = 0.03 and 0.06 for the *large* and *small models*, respectively. In addition, a vacuum slab that was 10 Å in length was attached to eliminate any interactions with the image cells. The H atoms were terminated at the Si atoms on the bottom surface to eliminate the effect of dangling bonds. The bottom Si layer including H atoms was fixed. These procedures aided in considering the simulation cell as an infinite bulk structure under the Si (110) surface. *k* point sampling was performed at 1 × 1 × 1 and 2 × 2 × 1 special points on the Monkhorst-Pack grid [15] for the *large* and *small models*, respectively.

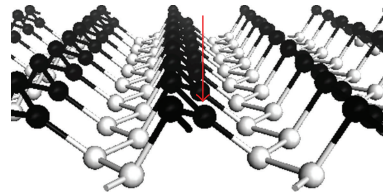

FIGURE 2: Atomic configuration of optimized Si (110)-(1 × 1) surface. Black (white) balls indicate the Si atoms in the first (second) layer.

The simulation cells were initially optimized. Then, the following three types of simulations were performed. In simulation (I), one or two O atoms were located at the A- and/or B-bond in both the *large* and *small models*, and the total energies of the optimized structures were calculated. This simulation gave us the information on the most stable site for situations including both one and two O atoms with different coverage ratios R_{ox}. In simulation (II), two *large models* were prepared. O atoms were located at all the A- and B-bonds in each model. After that, one O atom at the A-bond (B-bond) was eliminated from one (the other) model. Finally, the total energies of each model were calculated after the geometry optimization. The purpose of this simulation was to investigate the unoxidized bond when a coverage ratio of R_{ox} is close to 1.

The point defects play an important role in the Si oxidation process [16]. However, in this calculation, the formation of point defects was not considered as the stress easily releases due to the surface reconstruction in the initial stage of the oxidation.

3. Results and Discussion

Figure 2 shows part of the optimized Si (110)-(1 × 1) surface in the *small model*. We found that the surface structure, in

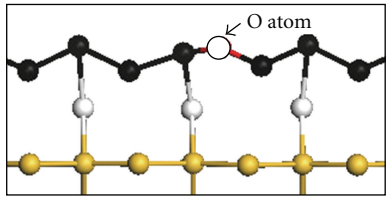

E_G = 8.57 eV

(a) A-bond

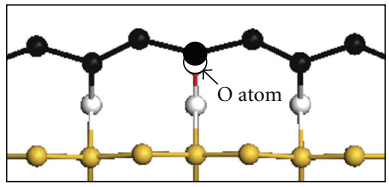

E_G = 8.12 eV

(b) B-bond

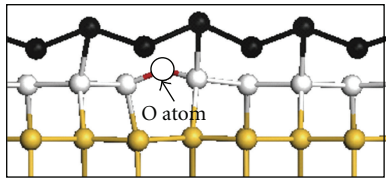

E_G = 7.96 eV

(c) A-bond in second layer

FIGURE 3: Cross sections of stable structures and energy gains E_G with O absorption at (a) A-bond, (b) B-bond, and (c) A-bond in second layer. Black (white) balls indicate the Si atoms in the first (second) layer. O atoms are indicated in each figure. The coverage ratio R_{ox} = 0.03.

which the Si atoms shown by the arrow in each zigzag line moved inward, was stable. This reconstructed surface agreed well with the results of the previous study using the first principles calculation [6].

3.1. Simulation (I)

3.1.1. The Most Stable Site of One O Atom. The total energy calculations were performed for the optimized *large* model including one O atom located at the A-bond, B-bond, and A-bond in the second layer. In this case, the coverage ratio was R_{ox} = 0.03. Figure 3 shows the cross sections of the stable structures and the energy gains with O absorption. Here, we obtained the energy gain E_G using (2):

$$E_G = (E_{tot}[(110)\ \text{surf}] + nE_O) - E_{tot}[O_n \text{ at } (110)\ \text{surf}]. \quad (2)$$

Here, $E_{tot}[(110)\ \text{surf}]$, E_O, and $E_{tot}[O_n$ at (110) surf] indicate the total energy of the optimized simulation cell of Si (110), the energy of one O atom, and the total energy of the cell including n number of O atoms, respectively. A positive E_G indicates there are stable O atoms on the (110) surface.

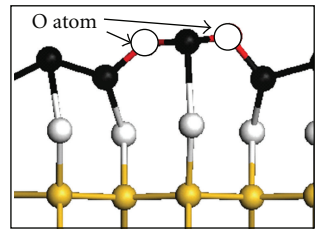

(a) O (A-bond) –Si–O (A-bond)

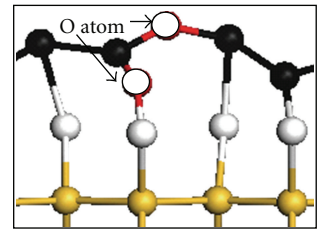

(b) O (A-bond) –Si–O (B-bond)

FIGURE 4: Cross sections of stable structures with absorption of two O atoms at (a) O (A-bond) –Si–O (A-bond) and (b) O (A-bond) –Si–O (B-bond). Black (white) balls indicate the Si atoms in the first (second) layer. O atoms are indicated in each figure. The coverage ratio R_{ox} = 0.10.

TABLE 1: Energy gains E_G with absorption of two O atoms.

Coverage ratio R_{ox}	Energy gain E_G		
	O (A-bond) –Si–O (A-bond)	O (A-bond) –Si–O (B-bond)	O (A-bond) –Si–Si–O (A-bond)
0.06	8.58 eV	8.47 eV	8.37 eV
0.10	8.44 eV	8.56 eV	8.26 eV

We found that the E_G at the A-bond was about 0.5 eV higher than that for the other sites. This indicates that the most stable site for one O atom is the A-bond in the first layer of the Si (110)-(1 × 1) surface. The change in the average length of the Si–Si bonds by O atom absorption was calculated. The obtained values for the O atom at the A-bond (B-bond) are 0.046 Å (0.045 Å) for the 1st neighbor Si–Si bonds from O atom and 0.006 Å (0.082 Å) for the 2nd neighbor Si–Si bonds from the O atom. This estimation indicates that the lattice strain around the O atom at the A-bond was smaller than that for the B-bond.

3.1.2. The Most Stable Site of Two O Atoms. The total energy calculations were performed for the *large* and *small models* including two O atoms. Figure 4 shows the typical stable structures with an absorption of two O atoms in the *small model*. Here, the coverage ratio was R_{ox} = 0.10. The energy gains E_G with the absorption of two O atoms are summarized in Table 1.

We found that (i) O (A-bond) –Si–O (A-bond) was most stable when R_{ox} = 0.06, while (ii) O (A-bond) –Si–O (B-bond) was most stable when R_{ox} = 0.10. The stability of the two O atoms for separated A-bonds (O (A-bond) –Si–Si–O (A-bond)) was less than these two structures as shown in this table. These results indicate that the O atoms will form clusters in the initial stage of oxidation, and furthermore, the stable site of the O atoms will shift from the A-bonds to the B-bonds with the progress of the oxidation. The O atom at the A-bond generates strain parallel to the surface, as shown in Figure 4(a). With an increase in the coverage ratio, this large strain accumulates due to the interaction with the O atoms in the image cells. On the other hand,

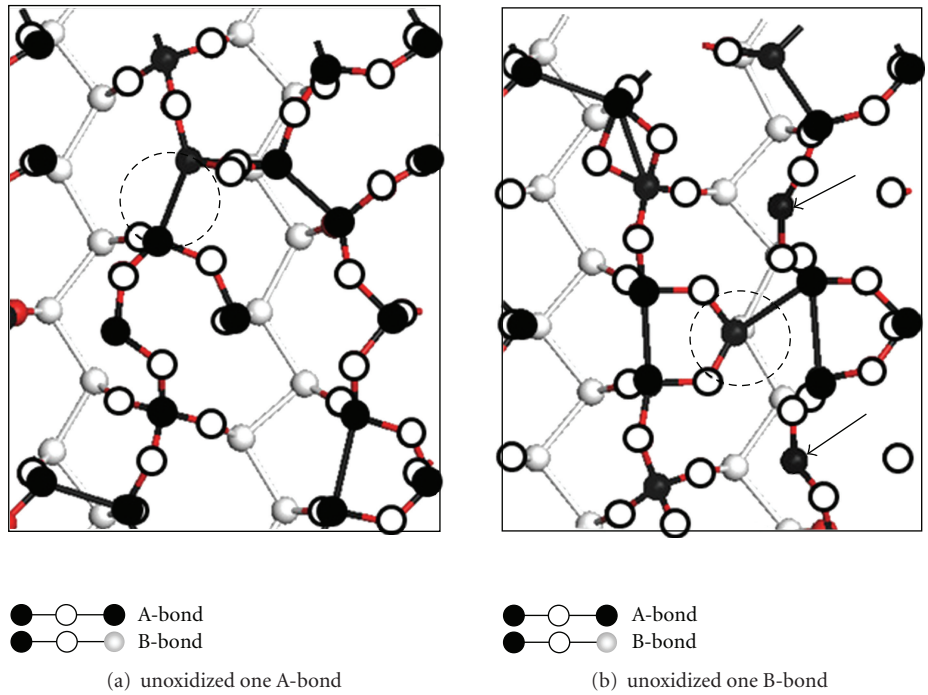

(a) unoxidized one A-bond (b) unoxidized one B-bond

Figure 5: Top views of obtained atomic configurations of cells including (a) unoxidized one A-bond and (b) unoxidized one B-bond. Black (white) balls indicate the Si atoms in the first (second) layer. The dotted circles indicate the unoxidized bonds. The Si atoms indicated by arrows in (b) moved outward at a large displacement.

the O atom at the B-bond moves the Si atoms in the first layer outward. In this case, the strain parallel to the surface will not accumulate that much. This results in a shift in the stable site of the O atoms from the A-bonds to the B bonds with an increase in the coverage ratio.

Si (110)-(1 × 1) surface was the most stable at higher than 700°C. It is thought that the structures in Figure 4 are stable even if they are quenched to a room temperature considering previous experimental reports [17].

3.2. Simulation (II). It is difficult to obtain the stable structures including some clusters of O atoms by first principles calculation. Therefore, in this simulation, the ideal models were used to estimate the unoxidized bonds left up to 1 ML oxide. First, two *large models* were prepared. The O atoms were located at all the A- and B-bonds in each model. After that, one O atom at the A-bond (B-bond) was eliminated from one (the other) of the models. Finally, the total energy of each model was calculated after geometry optimization. The possibility of the preferential oxidation was analyzed from those models. The coverage ratio R_{ox} of each model was 0.97. The top views of the obtained atomic configurations are shown in Figure 5. In this figure, the Si–Si bonds, at which the O atoms are eliminated, are shown by circles.

We found that the total energy of the cell including an unoxidized one A-bond was 5.22 eV less than that including an unoxidized one B-bond. In the Si (110)-(1 × 1) surface with an unoxidized one B-bond shown in Figure 5(b), the Si atoms indicated by arrows moved outward at a large displacement. We believe this large displacement is due to the large accumulated strain caused by the occupation of the O atoms at all A-bonds. Our results from simulations (I) and (II) suggest the preferential oxidation of the B-bonds with the progress of the oxidation and support the experimental results indicating that the dominant Si suboxide is Si^{3+} on a Si (110)-(1 × 1) surface up to 1 ML presented by Suemitsu et al [8].

4. Conclusion

We analyzed the initial stage of the oxidation of a Si (110)-(1 × 1) surface by using the first principles calculation. Two calculation cells with different surface areas were prepared. In these cells, O atoms were located at Si–Si bonds in the first layer (A-bonds) and at Si–Si bonds between the first and second layers (B-bonds). We found that (i) the most stable site of one O atom was the A-bond, and (ii) an O (A-bond) –Si–O (A-bond) is the most stable for two O atoms with a coverage ratio of $R_{ox} = 0.06$, while an O (A-bond) –Si–O (B-bond) is the most stable for $R_{ox} = 0.10$. The stability of O (A-bond) –Si–Si–O (A-bond) was less than the structures obtained in (ii). The other calculations showed that the unoxidized A-bonds should be left when a coverage ratio of R_{ox} is close to 1. These simulations suggest that the O atoms will form clusters in the initial stage of oxidation, and the preferential oxidation will change from the A-bonds to the B-bonds up to the formation of 1 monolayer (ML) oxide.

The results obtained here support the reported experimental results that the dominant Si suboxide is Si^{3+} on a Si (110)-(1 $\times$ 1) surface of up to 1 ML.

References

[1] M. Yang, V. W. C. Chan, K. K. Chan et al., "Hybrid-orientation technology (HOT): opportunities and challenges," *IEEE Transactions on Electron Devices*, vol. 53, no. 5, pp. 965–978, 2006.

[2] M. Yoshimura, T. An, and K. Ueda, "Observation of Si(110) surfaces by high-temperature scanning tunneling microscopy," *Japanese Journal of Applied Physics*, vol. 39, no. 7B, pp. 4432–4434, 2000.

[3] Y. Yamamoto, "Atomic arrangements of 16 $\times$ 2 and (17,15,1) 2 $\times$ 1 structures on a Si(110) surface," *Physical Review B*, vol. 50, no. 12, pp. 8534–8538, 1994.

[4] T. An, M. Yoshimura, I. Ono, and K. Ueda, "Elemental structure in Si(110)-"16 $\times$ 2" revealed by scanning tunneling microscopy," *Physical Review B*, vol. 61, no. 4, pp. 3006–3011, 2000.

[5] H. Togashi, Y. Tarahashi, A. Kato, A. Konno, H. Asaora, and M. Suemitsu, "Observation of initial oxidation on Si(110)-16 $\times$ 2 surface by scanning tunneling microscopy," *Japanese Journal of Applied Physics*, vol. 46, no. 5B, pp. 3239–3243, 2007.

[6] A. A. Stekolnikov, J. Furthmüller, and F. Bechstedt, "Long-range surface reconstruction: Si(110)-(16 $\times$ 2)," *Physical Review Letters*, vol. 93, no. 13, Article ID 136104, 4 pages, 2004.

[7] T. Nagasawa, S. Shiba, and K. Sueoka, "First-principles study on initial stage of oxidation on Si(110) surface," *Physica Status Solidi (c)*, vol. 8, no. 3, pp. 717–720, 2011.

[8] M. Suemitsu, Y. Yamamoto, H. Togashi, Y. Enta, A. Yoshigoe, and Y. Teraoka, "Initial oxidation of Si(110) as studied by real-time synchrotron-radiation X-ray photomission spectroscopy," *Journal of Vacuum Science and Technology B*, vol. 27, no. 1, pp. 547–550, 2009.

[9] "The *CASTEP* code," http://accelrys.com/.

[10] W. Kohn and L. J. Sham, "Self-consistent equations including exchange and correlation effects," *Physical Review*, vol. 140, no. 4A, pp. A1133–A1138, 1965.

[11] D. Vanderbilt, "Soft self-consistent pseudopotentials in a generalized eigenvalue formalism," *Physical Review B*, vol. 41, no. 11, pp. 7892–7895, 1990.

[12] J. P. Perdew, K. Burke, and M. Ernzerhof, "Generalized gradient approximation made simple," *Physical Review Letters*, vol. 77, no. 18, pp. 3865–3868, 1996.

[13] G. Kresse and J. Furthmüller, "Efficient iterative schemes for ab initio total-energy calculations using a plane-wave basis set," *Physical Review B*, vol. 54, no. 16, pp. 11169–11186, 1996.

[14] T. H. Fischer and J. Almlöf, "General methods for geometry and wave function optimization," *Journal of Physical Chemistry*, vol. 96, no. 24, pp. 9768–9774, 1992.

[15] H. J. Monkhorst and J. D. Pack, "Special points for Brillouin-zone integrations," *Physical Review B*, vol. 13, no. 12, pp. 5188–5192, 1976.

[16] H. Kageshima and K. Shiraishi, "First-principles study of oxide growth on Si(100) surfaces and at SiO_2/Si(100) interfaces," *Physical Review Letters*, vol. 81, no. 26, pp. 5936–5939, 1998.

[17] M. D. Pashley, K. W. Haberern, and W. Friday, "The effect of cooling rate on the surface reconstruction of annealed silicon(111) studied by scanning tunneling microscopy and low-energy electron diffraction," *Journal of Vacuum Science & Technology A*, vol. 6, no. 2, pp. 488–492, 1988.